THE JOURNAL OF BIOLOGICAL CHEMISTRY VOL. 284, NO. 47, pp. 32735–32741, November 20, 2009

Roles of Two Ca^{2+}-binding Domains in Regulation of the Cardiac Na^+-Ca^{2+} Exchanger*

Received for publication, August 12, 2009, and in revised form, September 22, 2009 Published, JBC Papers in Press, October 2, 2009, DOI 10.1074/jbc.M109.055434

Michela Ottolia[1], Debora A. Nicoll, and Kenneth D. Philipson

From the Department of Physiology and the Cardiovascular Research Laboratories, David Geffen School of Medicine, UCLA, Los Angeles, California 90095-1760

We expressed full-length Na^+-Ca^{2+} exchangers (NCXs) with mutations in two Ca^{2+}-binding domains (CBD1 and CBD2) to determine the roles of the CBDs in Ca^{2+}-dependent regulation of NCX. CBD1 has four Ca^{2+}-binding sites, and mutation of residues Asp^{421} and Glu^{451}, which primarily coordinate Ca^{2+} at sites 1 and 2, had little effect on regulation of NCX by Ca^{2+}. In contrast, mutations at residues Glu^{385}, Asp^{446}, Asp^{447}, and Asp^{500}, which coordinate Ca^{2+} at sites 3 and 4 of CBD1, resulted in a drastic decrease in the apparent affinity of peak exchange current for regulatory Ca^{2+}. Another mutant, M7, with 7 key residues of CBD1 replaced, showed a further decrease in apparent Ca^{2+} affinity but retained regulation, confirming a contribution of CBD2 to Ca^{2+} regulation. Addition of the mutation K585E (located in CBD2) into the M7 background induced a marked increase in Ca^{2+} affinity for both steady-state and peak currents. Also, we have shown previously that the CBD2 mutations E516L and E683V have no Ca^{2+}-dependent regulation. We now demonstrate that introduction of a positive charge at these locations rescues Ca^{2+}-dependent regulation. Finally, our data demonstrate that deletion of the unstructured loops between β-strands F and G of both CBDs does not alter the regulation of the exchanger by Ca^{2+}, indicating that these segments are not important in regulation. Thus, CBD1 and CBD2 have distinct roles in Ca^{2+}-dependent regulation of NCX. CBD1 determines the affinity of NCX for regulatory Ca^{2+}, although CBD2 is also necessary for Ca^{2+}-dependent regulation.

The Na^+-Ca^{2+} exchanger (NCX)[2] is a plasma membrane protein that uses the electrochemical gradient of Na^+ to extrude Ca^{2+} from cells (1). NCX is particularly abundant in cardiac myocytes and helps restore intracellular Ca^{2+} levels following excitation-contraction coupling (1). In addition to being transported substrates, cytoplasmic Na^+ and Ca^{2+} regulate NCX activity. Intracellular Na^+ decreases exchanger activity by inactivating NCX (Na^+-dependent inactivation or I_1), whereas cytoplasmic Ca^{2+} both stimulates activity and relieves the exchanger from the Na^+-dependent inactivation (2, 3). By tuning exchanger activity, regulation by Na^+ and Ca^{2+} has fundamental roles in Ca^{2+} homeostasis.

Regulatory Ca^{2+} binds to two cytoplasmic Ca^{2+}-binding domains (CBD1 and CBD2) located within the large intracellular loop of NCX, between transmembrane segments 5 and 6 (4–9). Each CBD comprises a β-sandwich containing seven antiparallel β-strands with Ca^{2+}-binding sites at one end of the β-sandwich (4, 5, 8, 9) and an unstructured loop connecting β-strands F and G at the opposite end of the sandwich. In CBD1, there are sites for coordinating four Ca^{2+} ions (Ca1–Ca4). Previous studies suggest that residues coordinating Ca^{2+} ions at sites 3 and 4 of CBD1 (10) set the affinity of the exchanger for cytoplasmic Ca^{2+}, whereas recent crystal and electrophysiological data show that binding of Ca1 is not required for exchanger regulation (11). No data are available on the role of Ca^{2+} bound at site 2.

Although the structure of CBD2 is similar to that of CBD1, it only contains sites for two Ca^{2+} ions (Ca1 and Ca2). Replacement of the residues responsible for coordinating Ca^{2+} at its primary site (Ca1) completely abolished Ca^{2+} regulation (4), indicating an important role for CBD2 in exchanger regulation. Ca^{2+} bound at the secondary site (Ca2) appears to have no role in exchanger regulation (4).

Despite recent progress, an understanding of the mechanisms leading to activation of NCX by cytoplasmic Ca^{2+} is still unresolved. It is well established that Ca^{2+} activates the exchanger by decreasing the extent of the Na^+-dependent inactivation and also by directly increasing NCX activity (2, 3). The relative contributions of CBD1 and CBD2 in the control of these mechanisms are unclear. To advance our understanding of Ca^{2+} regulation of the NCX, we mutated residues that coordinate Ca^{2+} in both domains and examined the effects on Ca^{2+}-dependent regulation. Our findings indicate that only Ca^{2+} sites 3 and 4 of CBD1 are important for Ca^{2+} regulation and that CBD2 also contributes to this process.

EXPERIMENTAL PROCEDURES

Mutagenesis and RNA synthesis were performed as described previously (12). RNAs encoding for NCXs were injected into *Xenopus laevis* oocytes. Oocytes were kept at 18 °C for 4–7 days. Inside-out giant patch recordings of outward NCX currents were performed as described previously (12, 13). Borosilicate glass pipettes of about 20–30 μm were utilized. Intracellular solutions were rapidly changed using a computer-controlled 20-channel solution switcher. Measurements were obtained using pipette solution (100 mM *N*-methylglucamine, 10 mM HEPES, 20 mM tetraethylammonium hydroxide, 0.2 mM

* This work was supported, in whole or in part, by National Institutes of Health Grant HL49101.

[1] To whom correspondence should be addressed: Cardiovascular Research Laboratory MRL 3-645, David Geffen School of Medicine, UCLA, Los Angeles, CA 90095-1760. Tel.: 310-825-5137; Fax: 310-206-5777; E-mail: mottolia@mednet.ucla.edu.

[2] The abbreviations used are: NCX, Na^+-Ca^{2+} exchanger; CBD, Ca^{2+}-binding domain; HEDTA, *N*-(2-hydroxyethyl)ethylenediamine-*N*,*N*′,*N*′-triacetic acid; I_1, Na^+-dependent inactivation; WT, wild type.

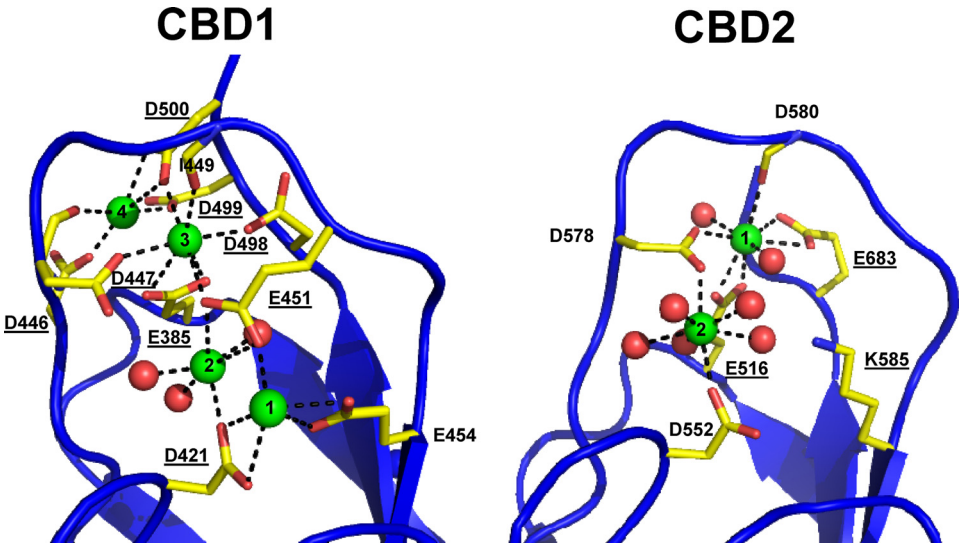

FIGURE 1. **Structures of the Ca^{2+}-binding sites of CBD1 and CBD2.** Shown are the organization of residues involved in coordinating Ca^{2+} ions in CBD1 (*left*) and CBD2 (*right*) (Protein Data Bank codes 2PDK and 2QVM). Residues mutated in this study are *underlined*.

niflumic acid, 0.2 mM ouabain, 8 mM $Ca(OH)_2$ (pH 7, adjusted with methanesulfonic acid)) and bath solution (100 mM CsOH or 100 mM NaOH, 20 mM tetraethylammonium hydroxide, 10 mM HEPES, 10 mM EGTA or HEDTA, and different $Ca(OH)_2$ concentrations to obtain the desired final free Ca^{2+} concentrations (pH 7, using methanesulfonic acid)). Free Ca^{2+} concentrations were calculated according to the WEBMAXC program (14) and confirmed with a Ca^{2+} electrode.

Ca^{2+} activation curves were obtained by perfusing solutions with different ion concentrations. Data were normalized to the maximum values and fitted to a Hill function. Each point is the average of between three and six experiments. Values are mean ± S.E. PCLAMP (Axon Instruments, Burlingame, CA) software was used for acquisition and analysis. Data were acquired on line at 4 ms/point and filtered at 50 Hz using an 8-pole Bessel filter. Experiments were performed at 35 °C and at a holding potential of 0 mV.

RESULTS

The crystal structures of the CBDs of the NCX have been resolved, and the regions involved in coordinating Ca^{2+} are shown in Fig. 1. Our goal was to determine the regulatory roles of specific Ca^{2+} ions that bind in CBD1 and CBD2. Residues mutated in this work are underlined. We utilized the giant patch technique (13) to characterize the response of mutant exchangers to cytoplasmic Ca^{2+}. Outward exchange currents were elicited by rapidly applying Na^+ (100 mM) into the bath at the intracellular surface of the patch. Ca^{2+} (8 mM) was continuously present within the pipette at the extracellular surface. As can be seen in the traces recorded from the wild type exchanger (WT) (Fig. 2*A*), exchange current peaks and then decays to a steady-state value when Na^+ is applied to the intracellular surface. The decay is triggered by the high intracellular Na^+ (Na^+-dependent inactivation or I_1). Increasing cytoplasmic Ca^{2+} concentrations increases the peak currents and antagonizes I_1 (3).

Mutations within CBD1—First, the effects of mutations within CBD1 were analyzed. Fig. 2 shows examples of WT, D421A, and E451A exchanger currents recorded at different intracellular Ca^{2+} concentrations. Asp^{421} and Glu^{451} are primarily involved in coordinating Ca^{2+} at Ca1 and Ca2 of CBD1 (Fig. 1). Similar to WT, currents recorded from oocytes expressing these mutants peaked rapidly and then decayed over several seconds because of the Na^+-dependent inactivation. Peak currents from both WT and mutant exchangers were enhanced by raising the intracellular concentration of regulatory Ca^{2+}. Because the onset of the Na^+-dependent inactivation is slow (3), the peak current reflects mainly the effects of Ca^{2+} on exchanger activation. Peak currents as a function of Ca^{2+} concentration for WT and mutant exchangers were fitted to a Hill function (Fig. 2*B*). The extrapolated values of the apparent Ca^{2+} affinities were 0.86 μM for the WT exchanger and 1.46 and 1.12 μM for D421A and E451A, respectively, indicating that mutations at these sites slightly reduce the sensitivity of NCX for cytoplasmic Ca^{2+}. In addition to activating the exchanger, increasing regulatory Ca^{2+} releases NCX from Na^+-dependent inactivation (2, 10). The effects of Ca^{2+} on Na^+-dependent inactivation are analyzed by measuring fractional currents calculated as the ratio of the steady-state current to the peak current (fractional activity). Both WT and D421A and E451A mutant exchangers show a similar reduction in the extent of Na^+-dependent inactivation with increasing Ca^{2+} (Fig. 2*C*), indicating that the mutations did not alter the effects of Ca^{2+} on Na^+ regulation. Overall, our data indicate that Ca1 and Ca2 of CBD1 contribute minimally to regulation of the exchanger by Ca^{2+}.

The roles of residues coordinating Ca^{2+} to sites 3 and 4 of CBD1 were also investigated. Residues Glu^{385}, Asp^{447}, Ile^{449}, Glu^{451}, Asp^{498}, and Asp^{500} coordinate Ca^{2+} at site 3, whereas Asp^{446}, Asp^{447}, Asp^{499}, and Asp^{500} comprise site 4. Single mutants D447V, D498I, and D500V were previously shown to alter markedly the apparent affinity of the exchanger for cytoplasmic Ca^{2+} (10). We now characterize the biophysical properties of two mutants E385A and double mutant D446A/D447A and further investigate the effects of replacing Asp^{500} with valine. Glu^{385} exclusively coordinates Ca^{2+} at site 3, whereas mutants D446A/D447A and D500V will perturb Ca^{2+} binding at both sites 3 and 4. Fig. 3 shows representative outward current traces recorded at the indicated regulatory Ca^{2+} concentrations from oocytes expressing the mutant exchangers. Activation of currents from E385A, double mutant D446A/D447A, and D500V required higher intracellular Ca^{2+} than did the WT exchanger. The dependence of the peak current on intracellular Ca^{2+} for WT and exchanger mutants is shown in Fig. 3*B*. Mutations at these sites decreased the apparent Ca^{2+}

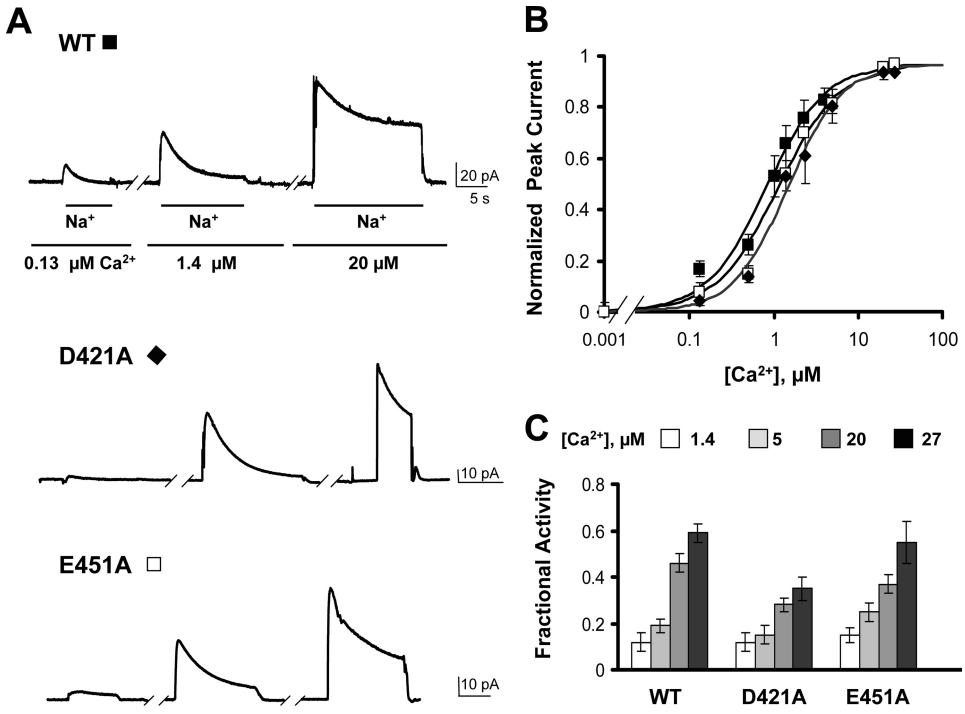

FIGURE 2. **Ca^{2+} ions coordinated by sites 1 and 2 of CBD1 are not essential for Ca^{2+} regulation.** *A*, examples of giant patch recordings from oocytes expressing the indicated construct. Outward currents were generated by rapidly applying 100 mM Na^+ into the bath (intracellular surface) with 8 mM Ca^{2+} in the pipette. Representative traces in the presence of three different intracellular Ca^{2+} concentrations are shown (0.13, 1.4, and 20 μM). Neither Na^+-dependent inactivation nor Ca^{2+} regulation is much affected by mutations at positions 421 or 451. *B*, Ca^{2+} dependence of outward exchanger current. Values were measured at the peak of the current. Residual current recorded in the absence of regulatory Ca^{2+} has been subtracted. Each point is the average of between two and six experiments. *C*, summary of the fractional activity values for the WT and the exchanger mutants measured in the presence of the indicated Ca^{2+} concentrations. Fractional activity was measured as the ratio between steady-state and peak currents. Each point is the average of between three and six experiments.

affinity of the exchanger by about 5-fold ($K_{1/2}$ micromolar values are 0.86, 3.51, 4.80, and 4.93 for WT, E385A, D446A/D447A, and D500V, respectively), indicating an important role for Ca^{2+} at CBD1 sites Ca3 and Ca4 in exchanger regulation.

Next, we constructed and characterized an exchanger with mutations in 7 of the 10 acidic amino acids (designated M7, with the following residues mutated to alanine: 385, 421, 446, 447, 498, 499, and 500) that are directly involved in the coordination of Ca^{2+} to CBD1. CBD1 of M7 should be incapable of binding Ca^{2+}. Although it was not possible to quantify the apparent Ca^{2+} affinity of peak currents because of lack of saturation, M7 retained Ca^{2+} regulation (Fig. 3, *A* and *B*), unmasking a role for CBD2 in exchanger regulation.

The effects of cytoplasmic Ca^{2+} on the Na^+-dependent inactivation of WT and exchanger mutants were then investigated. First, the fraction of inactivated mutant exchangers was quantified by measuring fractional activity. As shown in Fig. 3*C*, the fractional activity values measured for E385A, D446A/D447A, D500V, and M7 were significantly higher than that of WT (values are 0.12 ± 0.04 for WT, 0.28 ± 0.01 for E385A, 0.42 ± 0.06 for D446A/D447A, 0.47 ± 0.16 for D500V, and 0.35 ± 0.07 for M7, measured in the presence of 1.4 μM regulatory Ca^{2+}), indicating that the Na^+-dependent inactivation was less pronounced in the mutant exchangers.

To investigate Ca^{2+} regulation further, we examined the Ca^{2+} dependence of steady-state current. Ca^{2+} influences steady-state current by both increasing exchanger activity and relieving NCX from the Na^+-dependent inactivation. For the WT exchanger, the dependence of the steady-state current on Ca^{2+} is shifted to a much higher Ca^{2+} than the peak current (Fig. 4) (3). Fig. 4 also shows normalized peak and steady-state Ca^{2+} activation curves for mutants E385A and D500V. The gap between the concentration dependences of peak and steady-state currents for regulatory Ca^{2+} was significantly reduced in E385A mutant because of a decrease in Ca^{2+} sensitivity of the peak current. Interestingly, for mutant D500V, the steady-state current is saturable and shows a nearly identical affinity as the peak current. In this mutant, the affinity of the peak current is simultaneously reduced, and the sensitivity of the steady-state current to cytoplasmic $Ca^{2+}$is increased. The results emphasize the important role that Ca^{2+} ions coordinated by sites 3 and 4 of CBD1 play in exchanger regulation.

Mutations within CBD2—We next examined the effects of mutations within CBD2. Previously, we showed that three mutants within CBD2 (E516L, D578V, and E683V) lack Ca^{2+} regulation (4). These three anionic residues all contribute directly to the binding of the primary Ca^{2+} (Ca1) to CBD2. We refer to Ca1 of CBD2 as the primary Ca^{2+} because Ca2 is bound loosely and appears to have no function (4). We hypothesized that introducing a positive charge at these sites might partially mimic a Ca^{2+} ion and perhaps rescue Ca^{2+} regulation. Fig. 5 shows representative outward NCX currents for WT and mutants E516R and E683R in the absence and presence of Ca^{2+}. (Mutant D578R has been previously characterized and shown to be regulated by Ca^{2+} (15).) In the absence of regulatory Ca^{2+}, a substantial component of NCX current was present that was augmented by raising intracellular Ca^{2+}. Thus, the E516R and E683R mutants partially retained Ca^{2+} regulation of peak current in contrast to mutants in which neutral amino acids were used as replacements. Fig. 5*B* summarizes the effects of Ca^{2+} on peak currents, indicating that the Ca^{2+}-sensitive components of these mutants have apparent affinities for Ca^{2+} similar to those of WT ($K_{1/2}$ micromolar values are 0.86, 0.72, and 0.6 for WT, E516R, and E683R, respectively).

Fig. 5*C* shows a summary of the effects of Ca^{2+} on fractional activity of the WT and mutant exchangers. For WT, the extent of Na^+-dependent inactivation decreases as Ca^{2+} is elevated as indicated by increased fractional activity. As observed previously for mutants E516L, D578V, and E683V, introduction of a

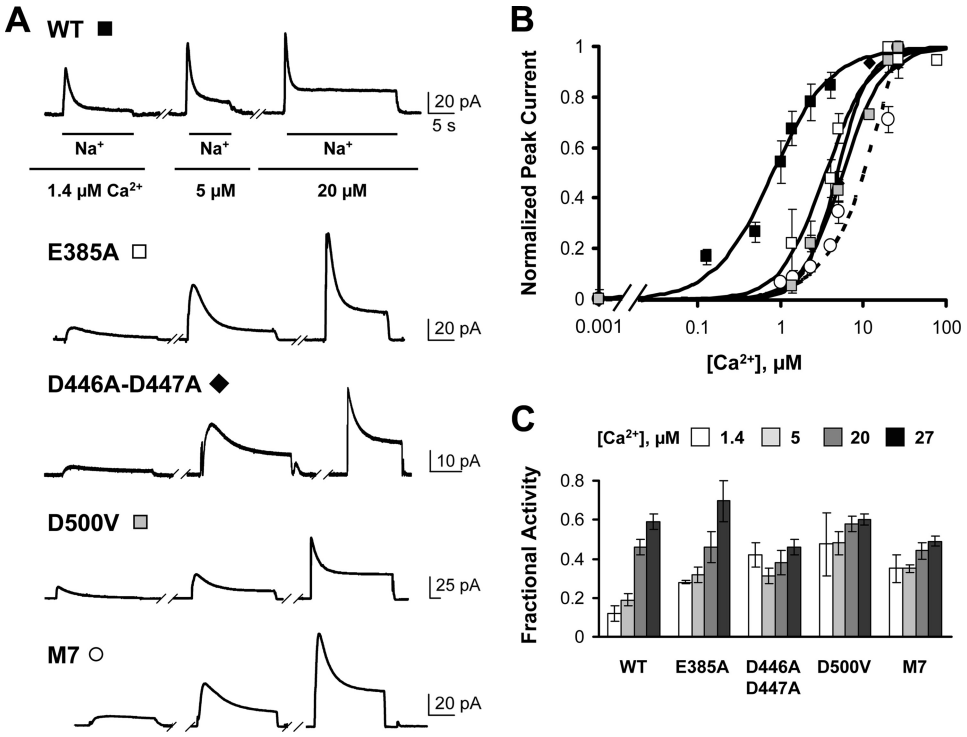

FIGURE 3. **Mutations of residues coordinating Ca^{2+} at sites 3 and 4 of CBD1 decrease the exchanger Ca^{2+} affinity.** *A*, representative outward currents recorded from oocytes expressing the indicated mutant. Residues Glu^{385}, Asp^{421}, Asp^{446}, Asp^{447}, Asp^{498}, Asp^{499}, and Asp^{500} of CBD1 were mutated to Ala in mutant M7. Notice that higher Ca^{2+} concentrations are required to activate the mutant exchangers. Ca^{2+} concentrations are shown below the *traces*. *B*, dose-response curves for cytoplasmic Ca^{2+} for WT and the indicated exchanger mutants. Current amplitudes were measured at peak currents. Residual current recorded in the absence of Ca^{2+} has been subtracted. Each point is the average of between two and four experiments. The M7 peak current was normalized at the highest concentration of Ca^{2+} examined because saturation was not obtained. *C*, fractional activity values for each exchanger. Measurements were done in the presence of the indicated Ca^{2+} concentrations.

positive charge at positions 516 and 683 disrupts the Ca^{2+} sensitivity of fractional activity.

Lys^{585} in CBD2 forms a salt bridge with Asp^{552} and Glu^{648} in the absence of Ca^{2+}, conferring structural integrity to the Ca^{2+}-free form (4). (Note that Glu^{683} of NCX1.1 studied here is equivalent to Glu^{648} of the splice variant NCX1.4 used in the crystallization studies.) Introduction of a negative charge at this location (K585E) slightly decreases the Ca^{2+} sensitivity of the peak current (4). There is also a marked alteration in the effect of Ca^{2+} on Na^+-dependent inactivation. The steady-state current becomes much more sensitive to intracellular Ca^{2+}. This can be seen in Fig. 6*A*, where 20 μM Ca^{2+} completely removes the Na^+-dependent inactivation of the K585E mutant, whereas this is not true of the WT exchanger (Figs. 2*A* and 3*A*; see also Fig. 6*C*).

We inferred above that the low affinity Ca^{2+} regulation of the CBD1 mutant M7 was due to CBD2. We tested that idea by introduction of the K585E mutation into the M7 background. If the K585E mutation does increase the affinity of CBD2 for Ca^{2+}, then it might partially rescue the low apparent Ca^{2+} affinity of M7. Indeed, this turns out to be the case. Addition of the mutation K585E into the M7 background resulted in an increase in apparent Ca^{2+} affinity of the peak current (Fig. 6*B*).

Role of the F-G Loops of CBD1 and CBD2 in Ca^{2+} Regulation of the Exchanger—The structures of CBD1 and CBD2 have been determined by both NMR and crystal structure (4–6, 8). Exceptions, however, are the long loops between β-strands F and G of both CBDs, which are unstructured. Although this F-G loop is well conserved among the CBD1 sequences of different exchangers, the corresponding amino acids of CBD2 vary substantially due to alternative splicing, resulting in CBD2s of varying length (16). To determine the functional role of these portions of the CBDs, we deleted residues 467–481 (CBD1) and 596–633 (CBD2) of NCX1.1 (mutant Δ(467–481)-(596–633)) to determine the effects on Ca^{2+} regulation. Fig. 7*A* shows outward currents recorded from oocytes expressing the exchanger carrying the double deletion. Similar to WT, exchange current peaked upon application of intracellular Na^+ and then was inactivated due to the high intracellular Na^+. Raising the intracellular Ca^{2+} concentration further activated the exchanger and decreased the extent of the Na^+-dependent inactivation. The fraction of steady-state to peak current values obtained for the WT and Δ(467–481)-(596–633) exchangers was not significantly different (Fig. 6*B*) (0.12 ± 0.04 and 0.46 ± 0.04 for WT and 0.18 ± 0.06 and 0.39 ± 0.06 for Δ(467–481)-(596–633), measured in the presence of 1.4 and 20 μM Ca^{2+}, respectively), indicating that these two regions of the exchanger are not important for Na^+-dependent inactivation. The effects of regulatory Ca^{2+} on peak outward current mediated by Δ(467–481)-(596–633) and WT exchangers are shown in Fig. 7*C*. Both exchangers exhibit a similar increase in the peak current as regulatory Ca^{2+} is raised. In summary, deletion of the F-G loops of CBD1 and CBD2 did not significantly alter the biophysical properties of the exchanger, indicating that these two unstructured regions do not play a fundamental role in secondary regulation of the exchanger by Ca^{2+}.

DISCUSSION

Regulatory Ca^{2+} modulates the activity of the NCX by binding to two cytoplasmic domains encompassing residues 371–501 (CBD1) and 501–678 (CBD2) (4–9, 17). CBD1 and CBD2 are both located within the large cytoplasmic loop of the exchanger between transmembrane segments 5 and 6 (7). Recently, the crystal structures of the exchanger CBDs have been resolved (4, 8, 9). CBD1 and CBD2 bind four and two Ca^{2+} ions, respectively. The domains have similar structures comprising seven antiparallel β-strands with the Ca^{2+}-binding sites within the connecting loops at one end of the structure. CBD1

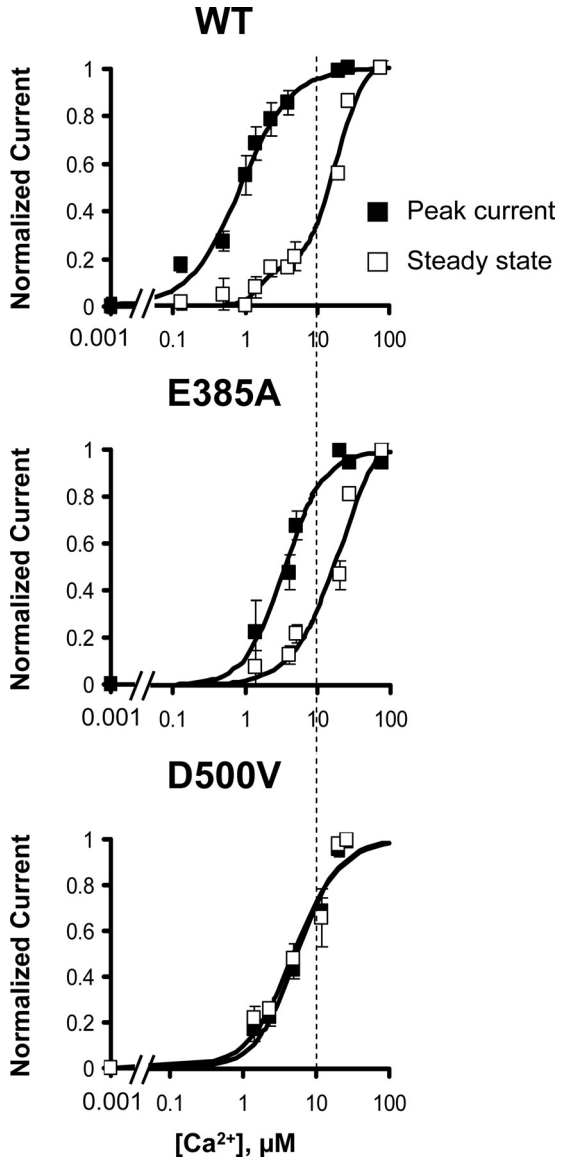

FIGURE 4. **Ca^{2+} sensitivities of peak and steady-state NCX currents.** Ca^{2+} dependences of outward current for peak (■) and steady-state (□) currents generated by WT and the indicated NCX mutants are shown. Note that, in contrast to WT, exchanger D500V shows the same affinity for Ca^{2+} for both peak and steady-state currents.

may undergo large conformational changes upon unbinding and binding of Ca^{2+} (5, 18, 19), although more constrained movements of CBD1 have also been reported (6). In contrast, CBD2 undergoes only minor structural rearrangements upon binding Ca^{2+} (4). CBD2 of the exchanger of *Drosophila melanogaster* does not appear to bind Ca^{2+} (9). Consistent with this observation, the *Drosophila* exchanger displays anomalous regulatory properties (20).

Binding of cytoplasmic Ca^{2+} to these domains triggers two measurable molecular processes: Ca^{2+} activates the exchange current and also rescues current from Na^+-dependent inactivation (1, 21). Experimentally, these effects are investigated by measuring the initial peak of exchange current and the steady state current, respectively. Because Na^+-dependent inactivation occurs over several seconds, the effects of Ca^{2+} on peak currents mainly reflect exchanger activation, whereas steady-state currents are a function of effects of Ca^{2+} on both exchanger activation and rescue from the Na^+-dependent inactivation. The conformational changes that drive these two regulations are unclear as are the contributions of each CBD. To elucidate the roles of CBD1 and CBD2, we mutated strategic residues within these two domains, guided by the crystal structures, and we determined their effects on Ca^{2+} regulation using electrophysiology. We first examined the effects of mutations within CBD1. Mutations of residues Asp^{421} and Glu^{451} minimally alter the Ca^{2+} sensitivity of NCX. These residues primarily coordinate Ca1 and Ca2. Thus, our data indicate that the Ca1 and Ca2 sites within CBD1 are not crucial in conferring Ca^{2+} regulation to the exchanger. These results are supported by recent structural and electrophysiological data showing that a mutant exchanger unable to bind Ca^{2+} at position 1 displays a phenotype similar to the WT exchanger (11).

Recent studies investigating the kinetics and equilibrium properties of Ca^{2+} binding to CBD1 and CBD2 detected two low affinity Ca^{2+} sites in CBD1 (22). Our data would suggest that these sites are Ca1 and Ca2. Because the Ca^{2+}-binding affinities for these sites are higher than 30 μM (22), they may not be occupied under the conditions in which our electrophysiological experiments were performed.

In sharp contrast to the mutations that disrupt the Ca1 and Ca2 sites of CBD1, mutations of residues involved in forming the binding sites for Ca3 and Ca4 (E385A, D446V–D447V, and D500V) drastically alter the Ca^{2+} sensitivity of NCX. The decrease of the apparent affinity for cytoplasmic Ca^{2+} observed in these mutants emphasizes their important role in Ca^{2+} regulation of the NCX.

A mutant of particular interest is D500V, which disrupts the binding of Ca^{2+} to sites 3 and 4 of CBD1. As shown in Fig. 4, the Ca^{2+} dose-response curves of the D500V peak and steady-state currents overlap. This observation reflects the fact that this mutation abolishes the sensitivity of the Na^+-dependent inactivation for Ca^{2+} as shown in Fig. 3*C*. Only the activation of the exchanger transport by Ca^{2+} is observed. D500V is the first single mutation within CBD1 known to alter the effects of Ca^{2+} on Na^+-dependent inactivation therefore revealing an influence of CBD1 in this process.

The recognition of a second CBD in NCX is recent, and the role of this domain is less studied. To gain insight into the function of CBD2 in controlling activity, we inactivated CBD1 by mutating 7 of the 10 amino acids that coordinate Ca^{2+} binding to CBD1. This M7 exchanger was still Ca^{2+}-regulated, though with decreased Ca^{2+} affinity. As we predict CBD1 of M7 cannot bind Ca^{2+}, the remaining Ca^{2+} sensitivity must reflect the binding of Ca^{2+} to CBD2. Because of competition between Ca^{2+} and Na^+ at the transport site, it was not possible to increase the intracellular Ca^{2+} concentration sufficiently to determine the apparent affinity of CBD2 for Ca^{2+} accurately. However, the apparent Ca^{2+} affinity of CBD2 was increased and saturation was achieved when the mutation K585E of CBD2 was introduced into the M7 background. Lys^{585} is near the Ca^{2+}-binding sites of CBD2, and its replacement with a negative charge increases the apparent affinity for Ca^{2+} to relieve Na^+-dependent inactivation (4) (Fig. 5). Introduction of the K585E mutation into the M7 background appears to

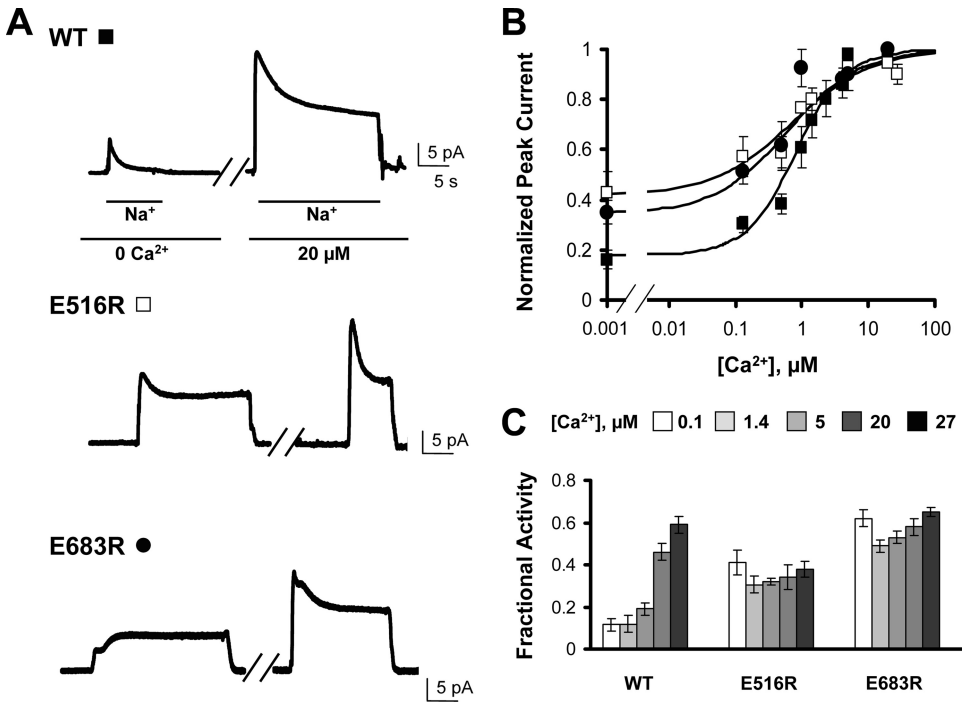

FIGURE 5. **Introduction of a positive charge at position 516 or 683 partially rescues NCX Ca^{2+} regulation.** Previously we have shown that NCX mutants E516L, D578V, and E683V lack Ca^{2+} regulation. Introduction of a positive charge at any of these positions partially restores NCX Ca^{2+} regulation. *A*, outward currents recorded from oocytes expressing the indicated construct. *B*, Peak current values *versus* cytoplasmic Ca^{2+} for WT (■), E516R (□), and E683R (●). *C*, fractional activity values measured at different Ca^{2+} concentrations for each exchanger.

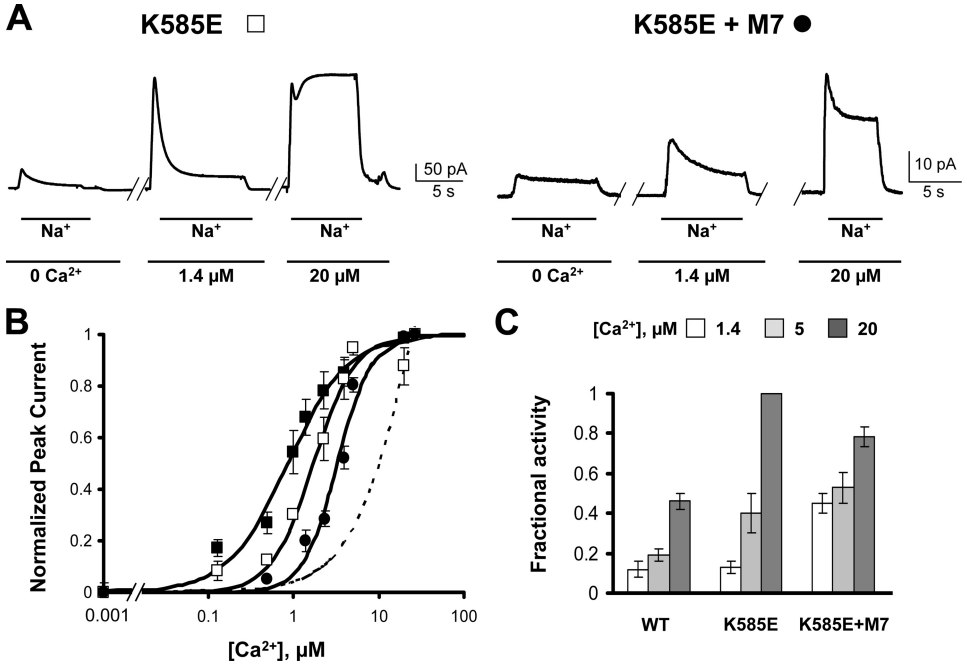

FIGURE 6. **Introduction of K585E into the NCX-M7 background increases apparent Ca^{2+} affinity.** *A*, outward currents recorded from excised patches of oocytes expressing the indicated construct. Bath [Ca^{2+}] is shown below the *traces*. *B*, peak current values *versus* cytoplasmic Ca^{2+} for WT (■), K585E (□), and K585E (●) in M7 background. The apparent affinities are 0.86 μM (WT), 1.7 μM (K585E), and 3.3 μM (K585E+M7). The *dashed line* shows the dose-response curve for Ca^{2+} for mutant M7 from Fig. 3. The apparent affinity of M7 for Ca^{2+} cannot be quantified due to lack of saturation. *C*, fractional activity values at different Ca^{2+} concentrations for each exchanger.

increase the Ca^{2+} affinity of CBD2, therefore conferring increased apparent Ca^{2+} affinity to M7. The result confirms that the Ca^{2+} regulation of M7 is due to CBD2. Alternatively, interactions between CBD1 and CBD2 may exist, and mutations in one CBD could affect the affinity of the other domain for Ca^{2+}.

To investigate further the role of CBD2 in controlling the Ca^{2+} regulation of the exchanger, two of the anionic amino acids (Glu^{516} and Glu^{683}) that coordinate the primary Ca^{2+} of CBD2 were replaced with positively charged lysines. Previously, we had shown that NCX mutants E516L, D578V, and E683V lack Ca^{2+} regulation (4). Introduction of a positive charge at any of these positions may mimic the presence of Ca^{2+} and therefore rescue Ca^{2+} regulation. Electrophysiological characterization of NCX mutant exchangers E516R and E683R revealed that indeed these mutants were regulated by Ca^{2+} with affinities similar to that of the WT exchanger. The mutant D578R has previously been shown to also be regulated by Ca^{2+} (15). Thus, it appears that a specific conformation of CBD2 is required to permit Ca^{2+} regulation to occur. This permissive conformation is provided by a positive charge at position 516 or 683 but not by substitution with a neutral amino acid. A functional CBD2 allows the Ca^{2+} affinity for regulation to be set by CBD1.

The structures of the domains of the exchanger that bind Ca^{2+} within the intracellular loop are known, with the exception of residues 467–481 and 596–633 within the F-G loops of CBD1 and CBD2, respectively. Because of high flexibility, the structure of these regions in the mammalian NCX remains undetermined. Likewise, their functional roles, if any, are unknown. Of particular interest are amino acid residues 596–633 (encoding exons C to F of NCX1.1) of CBD2 as this region varies greatly among exchanger isoforms due to alternative splicing (16). The use of alternative exons suggests a potential role of this region in exchanger regulation. For example, in the *Drosophila* NCX, which has anomalous inhibition by regulatory Ca^{2+}, the amino acid sequence of the F-G loop is quite different from NCX1, and the region is structured forming two helices in close proximity to the β-barrel structure of CBD2 (9). This region

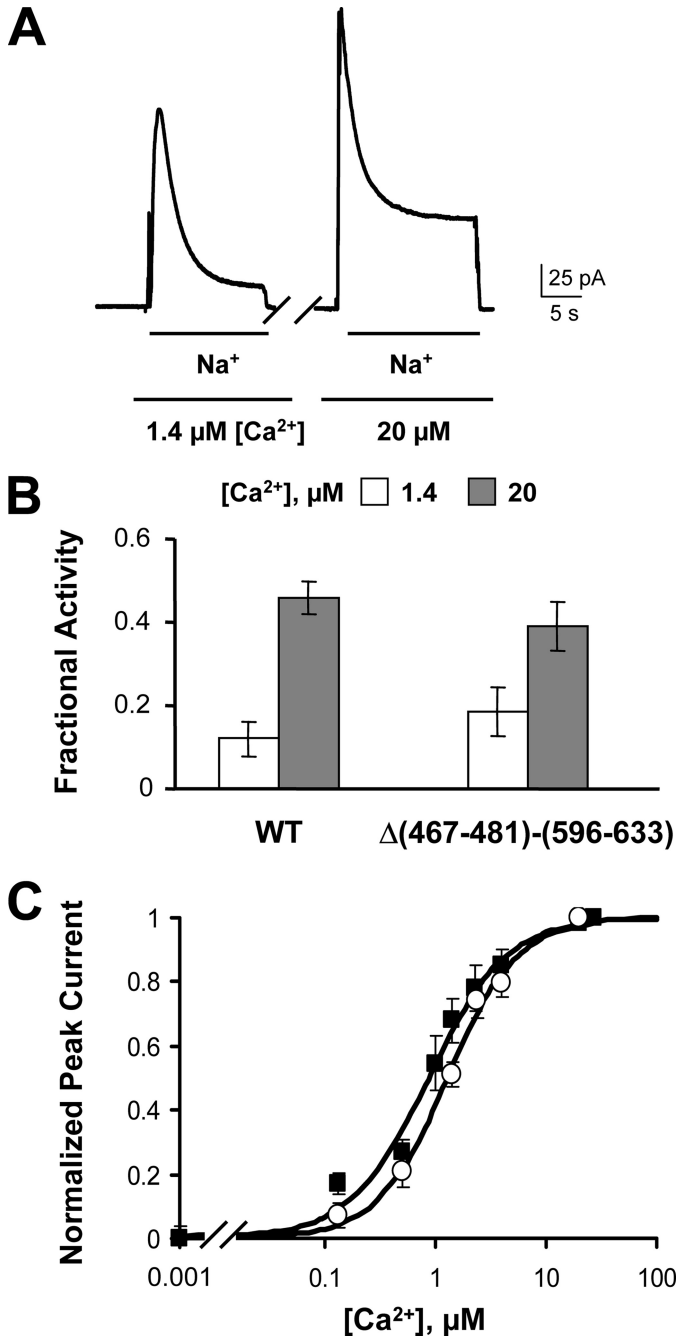

FIGURE 7. **Deletion of the F-G loops of CBD1 and CBD2 does not alter exchanger properties.** *A*, outward currents recorded from oocytes expressing NCX with residues 467–481 and 596–633 deleted. *B*, fractional activity values calculated from WT and Δ(467–481)-(596–633) currents recorded in the presence of 1.4 and 20 μM cytoplasmic Ca^{2+}. *C*, peak values *versus* cytoplasmic Ca^{2+} for WT (■) and the deletion mutant (○). The apparent affinity values for the regulatory Ca^{2+} dependence of peak current are 0.86 μM for WT and 1.28 μM for Δ(467–481)-(596–633).

may influence either the binding of Ca^{2+} to CBD1 or the transduction of the Ca^{2+} regulatory signal (9). We explored the contribution of the F-G loops to regulation of NCX1.1 by deletion and by characterizing the resultant mutant with respect to activation by cytoplasmic Ca^{2+}. Our data indicate that these portions of the CBD domains do not play any significant role in Ca^{2+} regulation.

In summary, our results indicate that both CBD1 and CBD2 contribute to the Ca^{2+} regulation of the NCX, although the exact roles of each domain are not completely resolved. Residues coordinating Ca^{2+} sites 3 and 4 in CBD1 and the primary Ca^{2+}-binding site (Ca1) in CBD2 are key in Ca^{2+} regulation and are involved in controlling both I_1 and I_2 processes. Further effort is needed to determine how CBD1 and CBD2 communicate with one another. Likewise, further studies are required to understand the transduction of the binding of regulatory Ca^{2+} to activation of the NCX.

Acknowledgment—We thank Dr. Vincent Chaptal for providing Fig. 1.

REFERENCES

1. Philipson, K. D., Nicoll, D. A., Ottolia, M., Quednau, B. D., Reuter, H., John, S., and Qiu, Z. (2002) *Ann. N. Y. Acad. Sci.* **976,** 1–10
2. Hilgemann, D. W., Collins, A., and Matsuoka, S. (1992) *J. Gen. Physiol.* **100,** 933–961
3. Hilgemann, D. W., Matsuoka, S., Nagel, G. A., and Collins, A. (1992) *J. Gen. Physiol.* **100,** 905–932
4. Besserer, G. M., Ottolia, M., Nicoll, D. A., Chaptal, V., Cascio, D., Philipson, K. D., and Abramson, J. (2007) *Proc. Natl. Acad. Sci. U.S.A.* **104,** 18467–18472
5. Hilge, M., Aelen, J., and Vuister, G. W. (2006) *Mol. Cell* **22,** 15–25
6. Johnson, E., Bruschweiler-Li, L., Showalter, S. A., Vuister, G. W., Zhang, F., and Brüschweiler, R. (2008) *J. Mol. Biol.* **377,** 945–955
7. Levitsky, D. O., Nicoll, D. A., and Philipson, K. D. (1994) *J. Biol. Chem.* **269,** 22847–22852
8. Nicoll, D. A., Sawaya, M. R., Kwon, S., Cascio, D., Philipson, K. D., and Abramson, J. (2006) *J. Biol. Chem.* **281,** 21577–21581
9. Wu, M., Wang, M., Nix, J., Hryshko, L. V., and Zheng, L. (2009) *J. Mol. Biol.* **387,** 104–112
10. Matsuoka, S., Nicoll, D. A., Hryshko, L. V., Levitsky, D. O., Weiss, J. N., and Philipson, K. D. (1995) *J. Gen. Physiol.* **105,** 403–420
11. Chaptal, V., Ottolia, M., Mercado-Besserer, G., Nicoll, D. A., Philipson, K. D., and Abramson, J. (2009) *J. Biol. Chem.* **284,** 14688–14692
12. Ottolia, M., Nicoll, D. A., and Philipson, K. D. (2005) *J. Biol. Chem.* **280,** 1061–1069
13. Hilgemann, D. W., and Lu, C. C. (1998) *Methods Enzymol.* **293,** 267–280
14. Patton, C., Thompson, S., and Epel, D. (2004) *Cell Calcium* **35,** 427–431
15. Dunn, J., Elias, C. L., Le, H. D., Omelchenko, A., Hryshko, L. V., and Lytton, J. (2002) *J. Biol. Chem.* **277,** 33957–33962
16. Quednau, B. D., Nicoll, D. A., and Philipson, K. D. (1997) *Am. J. Physiol. Cell Physiol.* **272,** C1250–C1261
17. Nicoll, D. A., Ottolia, M., and Philipson, K. D. (2002) *Ann. N. Y. Acad. Sci.* **976,** 11–18
18. Xie, Y., Ottolia, M., John, S. A., Chen, J. N., and Philipson, K. D. (2008) *Am. J. Physiol. Cell Physiol.* **295,** C388–C393
19. Ottolia, M., Philipson, K. D., and John, S. (2004) *Biophys. J.* **87,** 899–906
20. Hryshko, L. V., Matsuoka, S., Nicoll, D. A., Weiss, J. N., Schwarz, E. M., Benzer, S., and Philipson, K. D. (1996) *J. Gen. Physiol.* **108,** 67–74
21. Egger, M., and Niggli, E. (1999) *J. Membr. Biol.* **168,** 107–130
22. Boyman, L., Mikhasenko, H., Hiller, R., and Khananshvili, D. (2009) *J. Biol. Chem.* **284,** 6185–6193